PHYSICAL REVIEW D **85,** 095019 (2012)

Nondiagonal charged lepton Yukawa matrix: Effects on neutrino mixing in supersymmetry

Giovanna Cottin, Marco Aurelio Díaz, and Benjamin Koch

Departamento de Física, Pontificia Universidad Católica de Chile, Avenida Vicuña Mackenna 4860, Santiago, Chile

(Received 5 January 2012; published 23 May 2012)

It is known that the neutrino $U_{\rm PMNS}$ matrix contains the diagonalization of the mass matrix of the charged leptons. In this article we study the influence of a nondiagonal mass matrix for charged leptons on the neutrino phenomenology in two specific R-parity violating supersymmetric models. Our analytical and numerical results for those models reveal important corrections due to a nontrivial charged lepton sector. Especially sensitive are the solar and reactor mixing angles.

DOI: 10.1103/PhysRevD.85.095019 PACS numbers: 13.15.+g, 12.60.Jv

I. INTRODUCTION

Supersymmetric models which incorporate small violations of R parity [1] are of special interest in the context of neutrino phenomenology [2]. It has been shown that they can give rise to neutrino masses and mixing angles that are compatible with experimental data. In specific models this is achieved by either taking into account low scale gravity effects, or by including loop effects in the neutrino propagator [3–7].

While neutrino masses and mixings are considered ''new physics'' beyond the standard model (SM), the masses, mixing angles and phase of the other nine fermions are described, within the SM, by using 13 independent parameters. It has however been pointed out that in models motivated by supersymmetric gauge unification, the number of free parameters can be reduced to eight [8,9]. In those grand unified theories (GUT), also the lepton mass matrix is nondiagonal and therefore has to be diagonalized in order to reproduce the observed charged lepton masses m_e, m_μ, m_τ.

Given the success of those approaches, it is natural to seek the combination of the supersymmetric description for the neutrino sector with the supersymmetric description of the mass sector of the other fermions. The well-known neutrino $U_{\rm PMNS}$ matrix contains also a part that originates from the charged fermion mass sector, a fact which is studied in some cases [10,11], but neglected in most cases in the context of bilinear R-parity violation (BRpV). Given a nondiagonal charged lepton sector, a combination of the neutral and charged sectors is typically nontrivial. In this paper it will be studied how at low energy the GUT fermion mass matrices [8,9] affect the predictions of neutrino models with R-parity violation [5,6]. The models studied in the neutrino context are split supersymmetry (SS) and partial split supersymmetry (PSS), linked each to corresponding well known examples of charged lepton mass matrix textures. The conceptual frame of this combination of two viable and successful ideas and its realization in terms of explicit models is shown in Fig. 1. A priory there is no restriction when combining models for charged leptons with models for neutrinos. We decided to study two specific examples as shown in Fig. 1.

II. NEUTRAL AND CHARGED FERMIONS IN BRPV

In the supersymmetric models we are studying here, tree-level contributions to neutrino masses and mixings arise from the neutrino-neutralino mixing due to bilinear R-parity violation. In general, when writing down the gauge invariant terms that violate R parity one can consider Lagrange terms that contain three fields (trilinear) and terms that contain two fields (bilinear). In the context of SS all the trilinear terms are irrelevant since they contain heavy scalars that are integrated out of the effective theory.

In BRpV models neutralinos mix with neutrinos such that a 7×7 mass matrix is generated. In the base $\psi_0^T = (-i\tilde{B}, i\tilde{W}^0, \tilde{H}_d^0, \tilde{H}_u^0, \nu_e, \nu_\mu, \nu_\tau)$ the corresponding terms in the Lagrangian are grouped as

$$\mathcal{L}_N = -\tfrac{1}{2}(\psi^0)^T \mathcal{M}_N \psi^0, \tag{1}$$

with the mass matrix introduced in blocks [4],

$$\mathcal{M}_N = \begin{pmatrix} \mathrm{M}_{\chi^0} & m^T \\ m & 0 \end{pmatrix}, \tag{2}$$

This neutralino/neutrino mass matrix is diagonalized with the rotation matrix,

$$\begin{aligned}\mathcal{N} &= \begin{pmatrix} N & 0 \\ 0 & U_\nu^T \end{pmatrix}\begin{pmatrix} 1-\frac{1}{2}\xi^T\xi & \xi^T \\ -\xi & 1-\frac{1}{2}\xi\xi^T \end{pmatrix} \\ &\equiv \begin{pmatrix} N & 0 \\ 0 & U_\nu^T \end{pmatrix}\mathcal{N}_\xi, \end{aligned}\tag{3}$$

with $\xi = m\mathrm{M}_{\chi^0}^{-1}$ at first order in perturbation theory. The matrix $\mathcal{N}_\xi$ allows a block diagonalization such that

$$\mathcal{N}_\xi \mathcal{M}_N \mathcal{N}_\xi^T = \begin{pmatrix} \mathrm{M}_{\chi^0} & 0 \\ 0 & \mathrm{M}_\nu^{\rm eff} \end{pmatrix}, \tag{4}$$

with $\mathrm{M}_\nu^{\rm eff} = -m\mathrm{M}_{\chi^0}^{-1}m^T$. Matrices N and U_ν further diagonalize the neutralino mass matrix M_{χ^0} and the effective neutrino mass matrix $\mathrm{M}_\nu^{\rm eff}$, respectively,

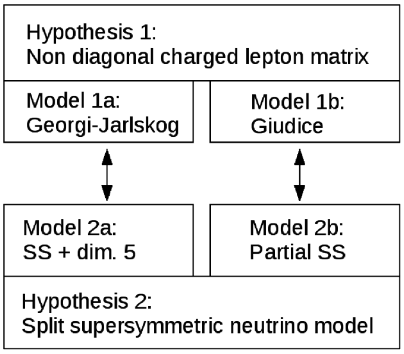

FIG. 1. Conceptual flow chart of how the basic ideas of a nondiagonal charge lepton Yukawa matrix and split supersymmetric neutrino models are combined and studied.

$$\begin{pmatrix} N & 0 \\ 0 & U_\nu^T \end{pmatrix}\begin{pmatrix} \mathcal{M}_{\tilde\chi^0} & 0 \\ 0 & \mathcal{M}_\nu^{\rm eff} \end{pmatrix}\begin{pmatrix} N^T & 0 \\ 0 & U_\nu \end{pmatrix} = \begin{pmatrix} \mathcal{M}_{\tilde\chi^0}^{\rm diag} & 0 \\ 0 & \mathcal{M}_\nu^{\rm diag} \end{pmatrix}. \quad (5)$$

We call these eigenstates F_i^0 with $i = 1, \ldots 7$.

As we will see, in order to correctly define the neutrino mixing angles we need to study the charged lepton sector as well. In BRpV charginos mix with charged leptons forming the following mass terms:

$$\mathcal{L}_C = -\frac{1}{2}(\psi^{+T}, \psi^{-T})\begin{pmatrix} 0 & \mathcal{M}_C^T \\ \mathcal{M}_C & 0 \end{pmatrix}\begin{pmatrix} \psi^+ \\ \psi^- \end{pmatrix}, \quad (6)$$

where the basis is $\psi^{-T} = (-i\tilde{W}^-, \tilde{H}_d^-, e_L^-, \mu_L^-, \tau_L^-)$ and $\psi^{-T} = (-i\tilde{W}^+, \tilde{H}_u^+, e_R^+, \mu_R^+, \tau_R^+)$. We divide the 5×5 mass matrix into blocks [4],

$$\mathcal{M}_C = \begin{pmatrix} M_{\chi^+} & Y \\ m_c & M_\ell \end{pmatrix}. \quad (7)$$

This chargino/charged lepton mass matrix is not symmetric thus it is diagonalized by two matrices:

$$\mathcal{U}\,\mathcal{M}_C\,\mathcal{V}^T = \mathcal{M}_C^{\rm diag}, \quad (8)$$

where we first look for a block diagonalization, as in the neutral case, performed by matrices $\mathcal{U}_\xi$ and $\mathcal{V}_\xi$. Neglecting Y (small Yukawa couplings and sneutrino vacuum expectation values) we find

$$\mathcal{U}_\xi = \begin{pmatrix} 1 - \frac{1}{2}\xi_L^T\xi_L & \xi_L^T \\ -\xi_L & 1 - \frac{1}{2}\xi_L\xi_L^T \end{pmatrix},$$
$$\mathcal{V}_\xi = \begin{pmatrix} 1 - \frac{1}{2}\xi_R^T\xi_R & \xi_R^T \\ -\xi_R & 1 - \frac{1}{2}\xi_R\xi_R^T \end{pmatrix}, \quad (9)$$

with $\xi_L = m_c M_{\chi^+}^{-1}$ and $\xi_R = M_\ell m_c M_{\chi^+}^{-1}(M_{\chi^+}^{-1})^T$. In the small lepton masses and small BRpV parameters approximation, ξ_R can be neglected. This implies that to first order on BRpV parameters the chargino and the charged lepton mass matrices are unchanged by the block diagonalization,

$$M_{\chi^+}^{\rm eff} = M_{\chi^+}, \qquad M_\ell^{\rm eff} = M_\ell. \quad (10)$$

The full diagonalization is accomplished with

$$\mathcal{U} = \begin{pmatrix} U & 0 \\ 0 & V_L \end{pmatrix}\mathcal{U}_\xi, \qquad \mathcal{V} = \begin{pmatrix} V & 0 \\ 0 & V_R \end{pmatrix}\mathcal{V}_\xi, \quad (11)$$

where

$$UM_{\chi^+}V^T = M_{\chi^+}^{\rm diag}, \qquad V_L M_\ell V_R^T = M_\ell^{\rm diag}. \quad (12)$$

The matrices $M_{\chi^+}^{\rm diag}$ and $M_\ell^{\rm diag}$ contain the final chargino and charged lepton masses. We call these eigenstates $F_i^\pm$ with $i = 1, \ldots 5$.

III. GUT MOTIVATED ANSATZ FOR CHARGED LEPTONS MASS MATRIX

Grand unified theories provide a well-motivated framework to study nondiagonal charged lepton mass matrices. The most studied grand unification gauge groups are $SU(5)$ and $SO(10)$, which break down to the SM gauge group $SU(3) \times SU(2) \times U(1)$. In addition, the GUT can be embedded into supersymmetry. In this context, different proposals for a charged lepton mass matrix are postulated at the GUT scale. In the following subsections we will study two GUT examples based on the two groups mentioned above.

A. Georgi-Jarlskog ansatz

We consider first the Georgi-Jarlskog ansatz [8] for the charged lepton mass matrix, introduced in the context of an $SU(5)$ GUT theory, and reanalyzed in [9] for a supersymmetric $SO(10)$ GUT group. Written in the notation of the later article, the charged lepton mass matrix depends on three parameters D, E, and F, which we assume real. We have

$$M_\ell = \frac{v}{\sqrt{2}}\begin{pmatrix} 0 & F & 0 \\ F & -3E & 0 \\ 0 & 0 & D \end{pmatrix}, \quad (13)$$

which essentially does not change after renormalization group equation (RGE) running effects. The matrix is proportional to v when the low energy theory contains only one Higgs doublet (for example, split supersymmetry). In the case it contains two Higgs doublets (for example partial split supersymmetry) the replacement $v \to v_d$ must be made.

If we assume E is positive, the eigenvalues are

$$m_{\ell_1} = \frac{v}{2\sqrt{2}}(-3E + \sqrt{9E^2 + 4F^2})$$
$$m_{\ell_2} = \frac{v}{2\sqrt{2}}(-3E - \sqrt{9E^2 + 4F^2}) \qquad m_{\ell_3} = \frac{v}{\sqrt{2}}D. \tag{14}$$

These eigenvalues, up to a possible sign, are equal to $m_e = 0.511$ MeV, $m_\mu = 105.7$ MeV, and $m_\tau = 1777$ MeV, respectively [12], fixing the parameters in the charged lepton Yukawa matrix to $F = 4.22 \times 10^{-5}$, $E = 2.01 \times 10^{-4}$, and $D = 1.02 \times 10^{-2}$.

It is clear that only one angle is enough to parametrize $M_\ell^{\rm diag} = V_L M_\ell V_R^T$. Since M_ℓ is symmetric, the diagonalization matrix has the following form:

$$V_L = V_R = \begin{pmatrix} \cos\alpha & \sin\alpha & 0 \\ -\sin\alpha & \cos\alpha & 0 \\ 0 & 0 & 1 \end{pmatrix}, \qquad \tan 2\alpha = \frac{2F}{3E}. \tag{15}$$

This angle is such that $|\sin\alpha| \approx 0.0695$.

B. Giudice ansatz

The second ansatz we consider was introduced by G. Giudice [13] in the context of supersymmetric GUT. The charged lepton mass matrix is

$$M'_\ell = \frac{v_d}{\sqrt{2}} \begin{pmatrix} 0 & F & 0 \\ F & -3E & 2E \\ 0 & 2E & D \end{pmatrix}, \tag{16}$$

whose Yukawa couplings do not change after running. The implications of this type of ansatz in terms of neutrino textures have been investigated in [14–16]. We will associate this ansatz with partial split supersymmetry, hence the mass matrix is proportional to v_d. The hierarchical nature of the charged lepton and quarks necessitates $F \ll E \ll D$. In this approximation we find the following eigenvalues:

$$m_{\ell_1} \approx \frac{v_d}{\sqrt{2}} \frac{F^2}{3E} \qquad m_{\ell_2} \approx \frac{v_d}{\sqrt{2}}\left(-3E - 4\frac{E^2}{D}\right)$$
$$m_{\ell_3} \approx \frac{v_d}{\sqrt{2}}\left(D + 4\frac{E^2}{D}\right). \tag{17}$$

Imposing the experimental values of the charged leptons into these results we find $Fc_\beta = 4.17 \times 10^{-5}$, $Ec_\beta = 1.97 \times 10^{-4}$, and $Dc_\beta = 1.02 \times 10^{-2}$. Note that these Yukawa parameters grow with $\tan\beta$. Notice also that the numerical value of the parameters F, E, and C differ only slightly with respect to the ones obtained for the previous ansatz (for $v = v_d \Leftrightarrow \cos\beta = 1$). This is related to the fact that the charged lepton masses are hierarchical.

The mass matrix M'_ℓ in Eq. (16) is diagonalized by the following matrix:

$$V'_L = V'_R \approx \begin{pmatrix} 1 & -\frac{F}{3E} & 0 \\ \frac{F}{3E} & 1 & \frac{2E}{D} \\ 0 & -\frac{2E}{D} & 1 \end{pmatrix}, \tag{18}$$

where we have neglected smaller terms. We parametrize this rotation matrix with two angles,

$$V'_L = \begin{pmatrix} \cos\alpha' & \sin\alpha' & 0 \\ -\sin\alpha' & \cos\alpha' & 0 \\ 0 & 0 & 1 \end{pmatrix} \begin{pmatrix} 1 & 0 & 0 \\ 0 & \cos\theta' & \sin\theta' \\ 0 & -\sin\theta' & \cos\theta' \end{pmatrix},$$
$$\tan 2\alpha' \approx \frac{2F}{3E}, \qquad \tan 2\theta' \approx -\frac{4E}{D}. \tag{19}$$

These angles are such that $|\sin\alpha'| \approx 0.070$ and $|\sin\theta'| \approx 0.036$. Notice that $V'_L(\theta' = 0, \alpha' = \alpha) = V_L(\alpha)$. There exist of course more models for the structure of the charged lepton matrix [17], but we will focus in our study on the two models mentioned above.

IV. $U_{\rm PMNS}$ AND W BOSON COUPLING TO FERMIONS

Charged and neutral fermion couplings to the W boson are essential for the $U_{\rm PMNS}$ matrix of neutrino mixing angles because they define the base where charged leptons are diagonal. In BRpV models the situation is complicated by the fact that charginos mix with charged leptons, as we saw in the previous chapter. The relevant coupling is

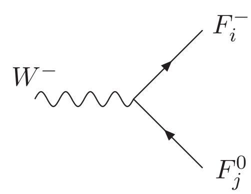

$$= i\gamma^\mu \left[O^{cnw}_{Lij} \frac{(1-\gamma_5)}{2} + O^{cnw}_{Rij} \frac{(1+\gamma_5)}{2} \right]$$

with

$$O^{cnw}_{Lij} = -g\left[\mathcal{N}_{j2} \mathcal{U}_{i1} + \frac{1}{\sqrt{2}}\left(\mathcal{N}_{j3} \mathcal{U}_{i2} + \sum_{k=1}^{3} \mathcal{N}_{j,4+k} \mathcal{U}_{i,2+k} \right) \right]$$
$$O^{cnw}_{Rij} = -g\left[\mathcal{N}_{j2} \mathcal{V}_{i1} + \frac{1}{\sqrt{2}} \mathcal{N}_{j4} \mathcal{V}_{i2} \right] \tag{20}$$

In first approximation in ϵ/M_χ we use

$$\mathcal{N} = \begin{pmatrix} N & N\xi^T \\ -U_\nu^T \xi & U_\nu^T \end{pmatrix}, \qquad \mathcal{U} = \begin{pmatrix} U & U\xi_L^T \\ -V_L \xi_L & V_L \end{pmatrix},$$
$$\mathcal{V} = \begin{pmatrix} V & 0 \\ 0 & V_R \end{pmatrix} \tag{21}$$

and find for the charged lepton and neutrino coupling to W Bosons the following:

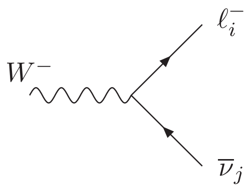

$$= -i \, \tfrac{g}{\sqrt{2}} \, (V_L U_\nu)_{ij} \, \gamma^\mu \, \tfrac{(1-\gamma_5)}{2}$$

Therefore, the neutrino mixing angles are defined by

$$U_{\mathrm{PMNS}} = V_L U_\nu. \tag{22}$$

Notice that the U_{PMNS} matrix coincides with the matrix that diagonalizes the neutrino mass matrix, U_ν, only when the charged leptons are diagonal in the original basis. Otherwise, there is an extra contribution from the left matrix V_L that diagonalizes the charged lepton mass matrix [11].

Using the following convention for the neutrino angles:

$$U_{\mathrm{PMNS}} = \begin{pmatrix} 1 & 0 & 0 \\ 0 & c_{23} & s_{23}e^{i\delta_{13}} \\ 0 & -s_{23}e^{-i\delta_{13}} & c_{23} \end{pmatrix} \times \begin{pmatrix} c_{13} & 0 & s_{13}e^{i\delta_{13}} \\ 0 & 1 & 0 \\ -s_{13}e^{-i\delta_{13}} & 0 & c_{13} \end{pmatrix} \times \begin{pmatrix} c_{12} & s_{12}e^{i\delta_{12}} & 0 \\ -s_{12}e^{-i\delta_{12}} & c_{12} & 0 \\ 0 & 0 & 1 \end{pmatrix} \tag{23}$$

and assuming this matrix is real ($\delta_{ij} = 0$), the general structure for the mixing angles considering the Giudice ansatz for the charged leptons (19) is given by

$$\begin{aligned} \sin\theta_{13}^{(V_L'\neq 1)} &= \sin\theta_{13}^{(V_L'=1)} + s_\alpha' s_{23} c_{13} \\ \tan\theta_{23}^{(V_L'\neq 1)} &= \tan\theta_{23}^{(V_L'=1)}\left\{1 + s_\theta'\left(t_{23} + \frac{1}{t_{23}}\right) - s_\alpha' \frac{t_{13}}{s_{23}}\right\} \\ \tan\theta_{12}^{(V_L'\neq 1)} &= \tan\theta_{12}^{(V_L'=1)}\left\{1 + s_\alpha' \frac{c_{23}}{c_{13}}\left(t_{12} + \frac{1}{t_{12}}\right)\right\}, \end{aligned} \tag{24}$$

where we have used the fact that the angles α' and θ' are small. A general form of this kind of expansion was given in [11]. Analogous expressions for the Georgi-Jarlskog ansatz are obtained by the substitution $V_L' \to V_L$, $\theta' = 0$, and $\alpha' \to \alpha$.

V. SPLIT SUPERSYMMETRY WITH FLAVOR BLIND DIMENSION FIVE

In split supersymmetry [18] all scalars are very heavy, for simplicity degenerated at a mass $\tilde{m}$, except for one Higgs doublet. Integrating out the heavy scalars the SS Lagrangian includes

$$\begin{aligned} \mathcal{L}_{\mathrm{SS}} \ni &-\left[m^2 H^\dagger H + \frac{\lambda}{2}(H^\dagger H)^2\right] - Y_u \bar{Q}_L u_R i\sigma_2 H^* \\ &- Y_d \bar{Q}_L d_R H - Y_e \bar{L}_L e_R H - \frac{M_3}{2}\tilde{G}\tilde{G} - \frac{M_2}{2}\tilde{W}\tilde{W} \\ &- \frac{M_1}{2}\tilde{B}\tilde{B} - \mu \tilde{H}_u^T i\sigma_2 \tilde{H}_d - \frac{1}{\sqrt{2}} H^\dagger(\tilde{g}_u \sigma \tilde{W} + \tilde{g}_u' \tilde{B})\tilde{H}_u \\ &- \frac{1}{\sqrt{2}} H^T i\sigma_2(-\tilde{g}_d \sigma \tilde{W} + \tilde{g}_d' \tilde{B})\tilde{H}_d + \mathrm{H.c.}, \end{aligned} \tag{25}$$

The last two terms are the Higgs-gaugino-Higgsino interactions, with couplings $\tilde{g}$ induced by integrating out the heavy scalars.

Split supersymmetry with violation of R parity [19] includes the extra terms

$$\mathcal{L}_{\mathrm{SS}}^{\mathrm{RpV}} \ni \epsilon_i \tilde{H}_u^T i\sigma_2 L_i - \frac{1}{\sqrt{2}} a_i H^T i\sigma_2(-\tilde{g}_d \sigma \tilde{W} + \tilde{g}_d' \tilde{B}) L_i + \mathrm{H.c.}. \tag{26}$$

The first term corresponds to the usual bilinear violation of R parity, which mixes Higgsinos with leptons through the mass parameters ϵ_i. The terms proportional to the a_i parameters are generated as effective terms in the SS Lagrangian after integrating out the sfermions.

A. Neutrinos and neutralinos in SS

Now we specify the neutrino-neutralino mixing described in Sec. II for the split supersymmetric case. The upper left block in Eq. (4) corresponds to the neutralino sector,

$$\mathbf{M}_{\chi^0}^{\mathrm{SS}} = \begin{pmatrix} M_1 & 0 & -\frac{1}{2}\tilde{g}_d' v & \frac{1}{2}\tilde{g}_u' v \\ 0 & M_2 & \frac{1}{2}\tilde{g}_d v & -\frac{1}{2}\tilde{g}_u v \\ -\frac{1}{2}\tilde{g}_d' v & \frac{1}{2}\tilde{g}_d v & 0 & -\mu \\ \frac{1}{2}\tilde{g}_u' v & -\frac{1}{2}\tilde{g}_u v & -\mu & 0 \end{pmatrix}, \tag{27}$$

where M_1, M_2 are the gaugino masses, μ is the Higgsino mass, and $v = 246$ GeV is the Higgs vacuum expectation value. The neutralino/neutrino mixing is equal to

$$m^{\mathrm{SS}} = \begin{pmatrix} -\frac{1}{2}\tilde{g}_d' a_1 v & \frac{1}{2}\tilde{g}_d a_1 v & 0 & \epsilon_1 \\ -\frac{1}{2}\tilde{g}_d' a_2 v & \frac{1}{2}\tilde{g}_d a_2 v & 0 & \epsilon_2 \\ -\frac{1}{2}\tilde{g}_d' a_3 v & \frac{1}{2}\tilde{g}_d a_3 v & 0 & \epsilon_3 \end{pmatrix}, \tag{28}$$

with ϵ_i and a_i the BRpV parameters described in Eq. (26). Therefore, in split supersymmetry the effective neutrino mass matrix is given by

$$\begin{aligned} \mathbf{M}_\nu^{\mathrm{eff}} &= -m^{\mathrm{SS}}(\mathbf{M}_{\chi^0}^{\mathrm{SS}})^{-1}(m^{\mathrm{SS}})^T \\ &= \frac{v^2}{4\det M_{\chi^0}^{\mathrm{SS}}}(M_1\tilde{g}_d^2 + M_2\tilde{g}_d'^2)\begin{pmatrix} \lambda_1^2 & \lambda_1\lambda_2 & \lambda_1\lambda_3 \\ \lambda_2\lambda_1 & \lambda_2^2 & \lambda_2\lambda_3 \\ \lambda_3\lambda_1 & \lambda_3\lambda_2 & \lambda_3^2 \end{pmatrix}, \end{aligned} \tag{29}$$

with $\lambda_i = a_i\mu + \epsilon_i$. The determinant of the neutralino mass matrix is found to be

$$\det M^{SS}_{\chi^0} = -\mu^2 M_1 M_2 + \tfrac{1}{2}v^2\mu(M_1\tilde{g}_u\tilde{g}_d + M_2\tilde{g}'_u\tilde{g}'_d) + \tfrac{1}{16}v^4(\tilde{g}'_u\tilde{g}_d - \tilde{g}_u\tilde{g}'_d)^2. \quad (30)$$

For our numerical calculations we neglect the running of the $\tilde{g}$ couplings.

Since the effective neutrino mass matrix has only one nonzero eigenvalue, at tree level only the atmospheric mass squared is generated, and the solar mass squared difference remains null. In split supersymmetry this does not change when we add quantum corrections to the neutrino mass matrix. This is a well-known fact in BRpV split supersymmetry [20]. Nevertheless, it has been noticed that gravity contributions via dimension-five operators, can generate a solar mass when the operator is suppressed by a reduced Planck mass, as in models with extra dimensions [21]. Following Ref. [5], we include a contribution to the neutrino mass matrix induced by gravity,

$$M_\nu^G = \mu_g \begin{pmatrix} 1 & 1 & 1 \\ 1 & 1 & 1 \\ 1 & 1 & 1 \end{pmatrix}, \quad (31)$$

where $\mu_g \sim v^2/M_X$ parametrizes the size of the contribution. This parameter has units of mass, is proportional to the Higgs vacuum expectation value squared v^2, and inversely proportional to the reduced Planck mass M_X. The equality of all entries in the matrix symbolizes the expected flavor blindness of the gravitational interactions.

Assuming that the charged lepton mass matrix is already diagonal, it was shown in Ref. [5] that neutrino mass squared differences predict values $\mu_g \sim 3\times 10^{-3}$ eV. This corresponds to a reduced Planck mass $M_X \sim 2\times 10^{16}$ GeV, remarkably close to the GUT mass scale. In addition, maximal atmospheric mixing predicts $\sin^2\theta_{\rm sol} = 1/3$, well within the 3σ experimental result $\sin^2\theta_{\rm sol} = 0.305 \pm 0.075$. In the following we will explore the effects of a nondiagonal charged lepton mass matrix.

B. Charged leptons and charginos in SS

In SS the chargino block in Eq. (7) has the following structure:

$$M_{\chi^+} = \begin{pmatrix} M_2 & \frac{1}{\sqrt{2}}\tilde{g}_u v \\ \frac{1}{\sqrt{2}}\tilde{g}_d v & \mu \end{pmatrix}, \quad (32)$$

with all the parameters already defined in the previous sections. The charged lepton mass matrix has the usual form $M_\ell^{ij} = Y_\ell^{ij} v/\sqrt{2}$, with Y_ℓ the lepton Yukawa couplings.

The mixing between charginos and charged leptons is given by the matrices

$$m_c = \begin{pmatrix} \frac{1}{\sqrt{2}}\tilde{g}_d a_1 v & -\epsilon_1 \\ \frac{1}{\sqrt{2}}\tilde{g}_d a_2 v & -\epsilon_2 \\ \frac{1}{\sqrt{2}}\tilde{g}_d a_3 v & -\epsilon_3 \end{pmatrix} \quad (33)$$

and

$$Y = \begin{pmatrix} 0 & 0 & 0 \\ -\frac{1}{\sqrt{2}}Y_\ell^{1i}a_i v & -\frac{1}{\sqrt{2}}Y_\ell^{2i}a_i v & -\frac{1}{\sqrt{2}}Y_\ell^{3i}a_i v \end{pmatrix}. \quad (34)$$

Since lepton masses are so much smaller than chargino masses and R-parity violating terms a_i are also small, it is usually a good approximation to neglect the effect of the matrix Y, as we did in the diagonalization process in Sec. II.

Notice that the charged lepton Yukawa matrix does not need to be diagonal. This point is nontrivial, and has consequences on the neutrino mixing angles in our models as we will see in the next chapters.

C. Effects on neutrino parameters in SS

The effective neutrino mass matrix, including BRpV terms and a gravity induced contribution from a flavor blind dimension-five operator in models with extra dimensions, is

$$M_\nu^{ij} = A_\lambda \lambda^i\lambda^j + \mu_g. \quad (35)$$

It is obtained by summing Eqs. (29) and (31), with the coefficient A_λ being read from Eq. (29). The neutrino mass parameters are not changed by the charged lepton contributions [5],

$$\begin{aligned} \Delta m^2_{\rm sol} &= \mu_g^2\frac{|\vec{v}\times\vec{\lambda}|^4}{|\vec{\lambda}|^4} + \mathcal{O}(\mu_g^3) \\ \Delta m^2_{\rm atm} &= A_\lambda^2|\vec{\lambda}|^4 + 2A_\lambda\mu_g(\vec{v}\cdot\vec{\lambda})^2 + \mathcal{O}(\mu_g^2), \end{aligned} \quad (36)$$

but the mixing angles are corrected. Considering the diagonalization matrix from Georgi-Jarlskog ansatz in Eq. (15), and using the convention in Eq. (23) for neutrino angles, we find

$$\begin{aligned} &\sin\theta_{13} = \frac{c\lambda_1 + s\lambda_2}{|\vec{\lambda}|} + \mathcal{O}(\mu_g) \qquad \tan\theta_{23} = \frac{c\lambda_2 - s\lambda_1}{\lambda_3} + \mathcal{O}(\mu_g) \\ &\tan\theta_{12} = \frac{1}{|\vec{\lambda}|}\left[\frac{c(\lambda_2^2+\lambda_3^2-\lambda_1\lambda_2-\lambda_1\lambda_3) + s(\lambda_1^2+\lambda_3^2-\lambda_1\lambda_2-\lambda_2\lambda_3)}{c(\lambda_3-\lambda_2)+s(\lambda_1-\lambda_3)}\right] + \mathcal{O}(\mu_g), \end{aligned} \quad (37)$$

where $c = \cos\alpha$ and $s = \sin\alpha$. These relations are a special case of the general formulae in Eq. (24).

From this we can learn the following. First, the 3σ upper bound $\sin^2\theta_{13} < 0.035$ [22] implies that a good approximation, as in [5], is $\lambda_1^2 \ll \lambda_2^2 + \lambda_3^2$. Therefore, the correction on $\sin^2\theta_{13}$ may be very significant since both terms in $c\lambda_1 + s\lambda_2$ are comparable. Second, the correction on the atmospheric angle is of a second order, since s and $\lambda_1/|\vec{\lambda}|$ are small. Third, the correction on the solar angle is typically of the order of s ($\sim 7\%$), which is non-negligible. In Sec. VII these effects are studied numerically.

VI. PARTIAL SPLIT SUPERSYMMETRY

In partial split supersymmetry all sfermions are heavy, for simplicity degenerate with a mass $\tilde{m}$, while the two Higgs doublets remain at the weak scale [6,19,23]. The Lagrangian includes

$$\begin{aligned}\mathcal{L}_{\rm PSS} \ni -\Big[& m_1^2 H_d^\dagger H_d + m_2^2 H_u^\dagger H_u - m_{12}^2 (H_d^T \epsilon H_u + \text{H.c.}) \\ & + \frac{1}{2}\lambda_1 (H_d^\dagger H_d)^2 + \frac{1}{2}\lambda_2 (H_u^\dagger H_u)^2 + \lambda_3 (H_d^\dagger H_d) \\ & \times (H_u^\dagger H_u) + \lambda_4 |H_d^T \epsilon H_u|^2 \Big] + Y_u \bar{u}_R H_u^T \epsilon q_L \\ & - Y_d \bar{d}_R H_d^T \epsilon q_L - Y_e \bar{e}_R H_d^T \epsilon l_L - \frac{1}{\sqrt{2}} H_u^\dagger (\tilde{g}_u \sigma \tilde{W} \\ & + \tilde{g}'_u \tilde{B}) \tilde{H}_u - \frac{1}{\sqrt{2}} H_d^\dagger (\tilde{g}_d \sigma \tilde{W} - \tilde{g}'_d \tilde{B}) \tilde{H}_d + \text{H.c.}\end{aligned} \tag{38}$$

The first two lines correspond to the Higgs potential of a two Higgs doublet model, where the quartic couplings have boundary conditions at $\tilde{m}$ that connect to the supersymmetric models above $\tilde{m}$. In the third line we include the Yukawa couplings, while in the forth one we have the Higgs-Higgsino-gaugino couplings. These Y and $\tilde{g}$ couplings in PSS differ from the corresponding ones in SS in their RGE and their boundary conditions at $\tilde{m}$.

BRpV is introduced in PSS with the terms,

$$\mathcal{L}_{\rm PSS}^{\rm RpV} = \epsilon_i \tilde{H}_u^T \epsilon L_i - \frac{1}{\sqrt{2}} b_i H_u^T \epsilon (\tilde{g}_d \sigma \tilde{W} - \tilde{g}'_d \tilde{B}) L_i + \text{H.c.}, \tag{39}$$

where the origin of the second term is analogous as in SS: they are generated as effective terms after integrating out the heavy sfermions.

A. Neutrinos and neutralinos in PSS

The neutralino sector of the neutrino/neutralino mass matrix in PSS has the following form:

$$\mathbf{M}_{\chi^0}^{\rm PSS} = \begin{pmatrix} M_1 & 0 & -\frac{1}{2}\tilde{g}'_d v_d & \frac{1}{2}\tilde{g}'_u v_u \\ 0 & M_2 & \frac{1}{2}\tilde{g}_d v_d & -\frac{1}{2}\tilde{g}_u v_u \\ -\frac{1}{2}\tilde{g}'_d v_d & \frac{1}{2}\tilde{g}_d v_d & 0 & -\mu \\ \frac{1}{2}\tilde{g}'_u v_u & -\frac{1}{2}\tilde{g}_u v_u & -\mu & 0 \end{pmatrix}. \tag{40}$$

It differs only slightly from SS in Eq. (27): it is apparent in Eq. (40) that there are two different vacuum expectation values, as in theminimal supersymmetric standard model, and as it was mentioned before the $\tilde{g}$ couplings have different RGE and boundary conditions. The mixing submatrix has also only minor differences,

$$m^{\rm PSS} = \begin{pmatrix} -\frac{1}{2}\tilde{g}'_d b_1 v_u & \frac{1}{2}\tilde{g}_d b_1 v_u & 0 & \epsilon_1 \\ -\frac{1}{2}\tilde{g}'_d b_2 v_u & \frac{1}{2}\tilde{g}_d b_2 v_u & 0 & \epsilon_2 \\ -\frac{1}{2}\tilde{g}'_d b_3 v_u & \frac{1}{2}\tilde{g}_d b_3 v_u & 0 & \epsilon_3 \end{pmatrix}. \tag{41}$$

The neutrino effective mass matrix in PSS takes the form,

$$\mathbf{M}_\nu^{\rm eff} = \frac{M_1 \tilde{g}_d^2 + M_2 \tilde{g}_d'^2}{4 \det M_{\chi^0}^{\rm PSS}} \begin{pmatrix} \Lambda_1^2 & \Lambda_1\Lambda_2 & \Lambda_1\Lambda_3 \\ \Lambda_2\Lambda_1 & \Lambda_2^2 & \Lambda_2\Lambda_3 \\ \Lambda_3\Lambda_1 & \Lambda_3\Lambda_2 & \Lambda_3^2 \end{pmatrix}, \tag{42}$$

with $\Lambda_i = \mu b_i v_u + \epsilon_i v_d$, and with the determinant of the neutralino submatrix equal to

$$\begin{aligned}\det M_{\chi^0}^{\rm PSS} = & -\mu^2 M_1 M_2 + \tfrac{1}{2} v_u v_d \mu (M_1 \tilde{g}_u \tilde{g}_d + M_2 \tilde{g}'_u \tilde{g}'_d) \\ & + \tfrac{1}{16} v_u^2 v_d^2 (\tilde{g}'_u \tilde{g}_d - \tilde{g}_u \tilde{g}'_d)^2.\end{aligned} \tag{43}$$

Despite these differences, the tree-level neutrino mass matrix in Eq. (42) also has only one nonzero eigenvalue, generating an atmospheric mass difference but not a solar mass difference. Nevertheless, as oppose to the SS case, in PSS quantum corrections do lift the symmetry of the tree-level matrix, generating a corrected neutrino mass matrix that looks like,

$$M_\nu^{ij} = A\Lambda_i\Lambda_j + C\epsilon_i\epsilon_j, \tag{44}$$

where the tree-level value $A^{(0)}$ can be read from Eq. (42). One-loop diagrams correct it into the value A, and generate the constant C. The matrix in Eq. (44) has only one null eigenvalue, thus a nonzero atmospheric and solar mass difference. A quadratic constant B that mixes Λ_i and ϵ_j is also generated in general, but can be adjusted to zero by choosing an appropriate value for the arbitrary renormalization scale of dimensional regularization.

This mechanism depends strongly on the b_i terms in the definition of Λ_i. The origin of those terms is that above the splitting scale $\tilde{m}$ the Higgs scalars gauge eigenstates mix with sneutrinos gauge eigenstates. This happens for the CP-even real parts and the CP-odd imaginary parts. Because of this mixing one might define the real part of sneutrinos (s_s^i, t_s^i) in the CP-even Higgs mass eigenstates (h, H). It has been shown that for the real part

$s_s^i \sim -b_i c_\alpha \sim -c_\alpha v_i/v_u$ and that $t_s^i \sim -b_i s_\alpha \sim -s_\alpha v_i/v_u$. The relations for the imaginary parts are analogous [19]. Thus, the existence of a nonzero b_i term in indicates that actually Higgs Bosons, at any energy scale below $\tilde{m}$ will have a small sneutrino component. This means that the original sneutrinos (interaction eigenstates) are not completely decoupled at those scales. It is further instructive to notice that the b_i are proportional to the sneutrino vacuum expectation value, which implies that it disappears for a restored $SU(2)$ symmetry. This fact is important in order to understand this model in context of some general theorems on neutrino masses [24,25].

B. Charged leptons and charginos in PSS

The chargino block in PSS has the following structure:

$$M_{\chi^+} = \begin{pmatrix} M_2 & \frac{1}{\sqrt{2}}\tilde{g}_u v_u \\ \frac{1}{\sqrt{2}}\tilde{g}_d v_d & \mu \end{pmatrix}. \tag{45}$$

The difference with the SS case in Eq. (32) lies in the fact that now we have two vacuum expectation values v_u and v_d (as in the minimal supersymmetric standard model), and that the $\tilde{g}$ couplings, defined in Eq. (38), are numerically different.

The mixing between charginos and charged leptons is given by the matrices

$$m_c = \begin{pmatrix} \frac{1}{\sqrt{2}}\tilde{g}_d b_1 v_d & -\epsilon_1 \\ \frac{1}{\sqrt{2}}\tilde{g}_d b_2 v_d & -\epsilon_2 \\ \frac{1}{\sqrt{2}}\tilde{g}_d b_3 v_d & -\epsilon_3 \end{pmatrix} \tag{46}$$

and

$$Y = \begin{pmatrix} 0 & 0 & 0 \\ -\frac{1}{\sqrt{2}} Y_\ell^{\prime 1i} b_i v_d & -\frac{1}{\sqrt{2}} Y_\ell^{\prime 2i} b_i v_d & -\frac{1}{\sqrt{2}} Y_\ell^{\prime 3i} b_i v_d \end{pmatrix}, \tag{47}$$

where Y' is the charged lepton Yukawa matrix in our second ansatz. The dimensionless parameter b_i plays the same role as a_i in SS.

As in SS, in this scenario we consider the charged lepton Yukawa coupling matrix as nondiagonal, and we consider its effect in the relation between neutrino parameters and observables.

C. Effects on neutrino parameters in PSS

The neutrino mass matrix in PSS is given by Eq. (44), and in what we call tree-level dominance scenario, defined by $A^2|\vec{\Lambda}|^4 \gg C^2|\vec{\epsilon}|^4$, the neutrino mass differences are found to be

$$\Delta m^2_{\text{atm}} \approx A^2|\vec{\Lambda}|^4, \qquad \Delta m^2_{\text{sol}} \approx C^2 \frac{|\vec{\epsilon} \times \vec{\Lambda}|^4}{|\vec{\Lambda}|^4}. \tag{48}$$

These expressions are not changed by the presence of a nontrivial diagonalization matrix V_L for the charged lepton mass matrix.

The three normalized eigenvectors of the neutrino mass matrix in Eq. (44) in the tree-level dominance scenario are, in first approximation,

$$\vec{e}_1 = \frac{\vec{\epsilon} \times \vec{\Lambda}}{|\vec{\epsilon} \times \vec{\Lambda}|}, \qquad \vec{e}_2 = \frac{\vec{\Lambda} \times (\vec{\epsilon} \times \vec{\Lambda})}{|\vec{\Lambda} \times (\vec{\epsilon} \times \vec{\Lambda})|}, \qquad \vec{e}_3 = \frac{\vec{\Lambda}}{|\vec{\Lambda}|}, \tag{49}$$

and they form the columns of the U_ν matrix. The neutrino mixing angles written in terms of the approximated mixing angles (when $V_L = 1$) are displayed in Eq. (24), while their expressions written in terms of the BRpV parameters [analogous to Eq. (37)] are more involved, and we display them in terms of the eigenvector components, and in the approximation $\sin\theta'$, $\sin\alpha' \ll 1$,

$$\begin{aligned} \sin\theta_{13} &= e_{31} + s_{\alpha'} e_{32} \qquad \tan\theta_{23} \\ &= \frac{e_{32}}{e_{33}}\left[1 + s_{\theta'}\left(\frac{e_{32}}{e_{33}} + \frac{e_{33}}{e_{32}}\right) - s_{\alpha'}\frac{e_{31}}{e_{32}}\right] \\ \tan\theta_{12} &= \frac{e_{21}}{e_{11}}\left[1 + s_{\alpha'}\left(\frac{e_{22}}{e_{21}} - \frac{e_{12}}{e_{11}}\right)\right], 1 \end{aligned} \tag{50}$$

where e_{ij} refers to the component j of the eigenvector $\vec{e}_i$. The numerical effect will be shown in the next section.

VII. NUMERICAL RESULTS

In this analysis, prediction of neutrino parameters is done by using numerical methods to find the eigenvalues and eigenvectors that correspond to U_ν and V_L. Using them, we find neutrino mass differences and mixing angles, and compare them with values from experimental measurements. We also study how a nondiagonal Yukawa matrix can influence the neutrino observables, specifically neutrino mixing angles.

The agreement with the experimental boundaries at the 3σ-level was quantified by calculating [22,26,27]

$$\begin{aligned} \chi^2 = &\left(\frac{10^3\Delta m^2_{\text{atm}} - 2,45}{0,31}\right)^2 + \left(\frac{10^5\Delta m^2_{\text{sol}} - 7,64}{0,55}\right)^2 \\ &+ \left(\frac{\sin^2\theta_{\text{atm}} - 0,515}{0,125}\right)^2 + \left(\frac{\sin^2\theta_{\text{sol}} - 0,315}{0,045}\right)^2 \\ &+ \left(\frac{\sin^2\theta_{\text{rea}} - 0,018}{0,017}\right)^2, \end{aligned} \tag{51}$$

where $\theta_{\text{atm}} = \theta_{23}$, $\theta_{\text{sol}} = \theta_{12}$, and $\theta_{\text{reac}} = \theta_{13}$. We accept values of $\chi^2 < 1$ to be consistent with experimental results.

A. Split SUSY

Our parameter space in SS can be classified into four type of variables. First supersymmetric parameters like the bino mass M_1, the wino mass M_2, the Higgsino mass μ, and the ratio between vacuum expectation values $\tan\beta$, whose effect can be all concentrated into the parameter A_λ defined in Eq. (35). Second the BRpV parameters λ_i, which give rise to an atmospheric mass. Third the gravity

TABLE I. Solutions for the parameters. This values gives $\chi^2 = 0.356$.

SUSY parameters	Value	Scanned range	Units
M_1	177	[40, 500]	GeV
M_2	300	[80, 100]	GeV
$\vert\mu\vert$	392	[0, 1000]	GeV
$\tan\beta$	25.1	[2, 50]	$\cdots$
A	-3.53	$\cdots$	eV/GeV^4
BRpV parameters	Value	Scanned range	Units
Λ_1	0.0109	$[-1, 1]$	GeV^2
Λ_2	-0.0873	$[-1, 1]$	GeV^2
Λ_3	0.0814	$[-1, 1]$	GeV^2
Gravity parameter	Value	Scanned range	Units
μ_g	0.00291	[0,0.005]	eV

TABLE II. SS predictions for neutrino observables given the values in Table I, and $\sin\alpha \approx -0.0695$.

Observable	Solution	Units
$\Delta m^2_{\rm atm}$	2.44×10^{-3}	eV^2
$\Delta m^2_{\rm sol}$	7.61×10^{-5}	eV^2
$\sin^2\theta_{\rm atm}$	0.532	$\cdots$
$\sin^2\theta_{\rm sol}$	0.290	$\cdots$
$\sin^2\theta_{\rm rea}$	0.0195	$\cdots$

parameter μ_g responsible for a solar mass. Fourth the charged lepton GUT parameters E, F, D which define the angle α in Eq. (15).

We scan the parameter space varying randomly A_λ, the BRpV parameters λ_i, and the gravity parameter μ_g, looking for a solution with good prediction for the neutrino parameters. In order to compare easily with PSS we define $\Lambda_i = v_d \lambda_i$ and $A = A_\lambda / v_d^2$ for the SS case. As a working point we choose the numerical values given in Table I, with the values of M_1, M_2, μ, and $\tan\beta$ as an example of a set that leads to the corresponding value for A. The charged lepton GUT parameters are fixed to their values inferred by the Georgi-Jarlskog ansatz in Eq. (13), which lead to $\sin\alpha \approx -0.0695$ (Note that there is an ambiguity on the sign of $\sin\alpha$, and we have chosen the negative one as a working example). This solution is in good agreement with all neutrino observables, with the predictions shown in Table II.

In Fig. 2 (left) we plot the logarithm of χ^2 as contour regions in the Λ_1 and Λ_3 plane, with fixed values for all the other parameters as indicated in Table I, plus $\sin\alpha \approx -0.0695$. Good solutions to neutrino observables are represented by the white region, corresponding to $\chi^2 < 1$. We see that the contours are not symmetric under a Λ_1 sign change. This is due to the χ^2 term corresponding to the reactor angle in Eq. (51), and can be understood from Eq. (37). We see that the correction to the reactor angle due to a nondiagonal charged lepton mass matrix is large because, in addition to the fact that $|\sin\alpha| \ll \cos\alpha$, we also have $|\Lambda_2| \gg |\Lambda_1|$ compensating the previous disbalance. Therefore, $\sin\theta_{13}$ is not symmetric under a change in the sign of Λ_1 unless it is accompanied by a corresponding change in the sign of Λ_2.

In order to see the effect of the diagonalization of the charged lepton mass matrix, we compare the same effect as before but now setting $\sin\alpha = 0$, which is equivalent to a diagonal charged lepton mass matrix. This is done in Fig. 2 (right), where we have the analogous contour plot for χ^2. One sees that for the chosen point in parameter space, the allowed (white) region for the case $\sin\alpha \approx -0.0695$ (Fig. 2, left) is smaller than the corresponding region for the case $\sin\alpha = 0$ (Fig. 2, right). This means that points in parameter space consistent with neutrino observables when the diagonalization of the charged lepton mass matrix is neglected, can actually be inconsistent when this diagonalization is taken into account (Of course, this has been done

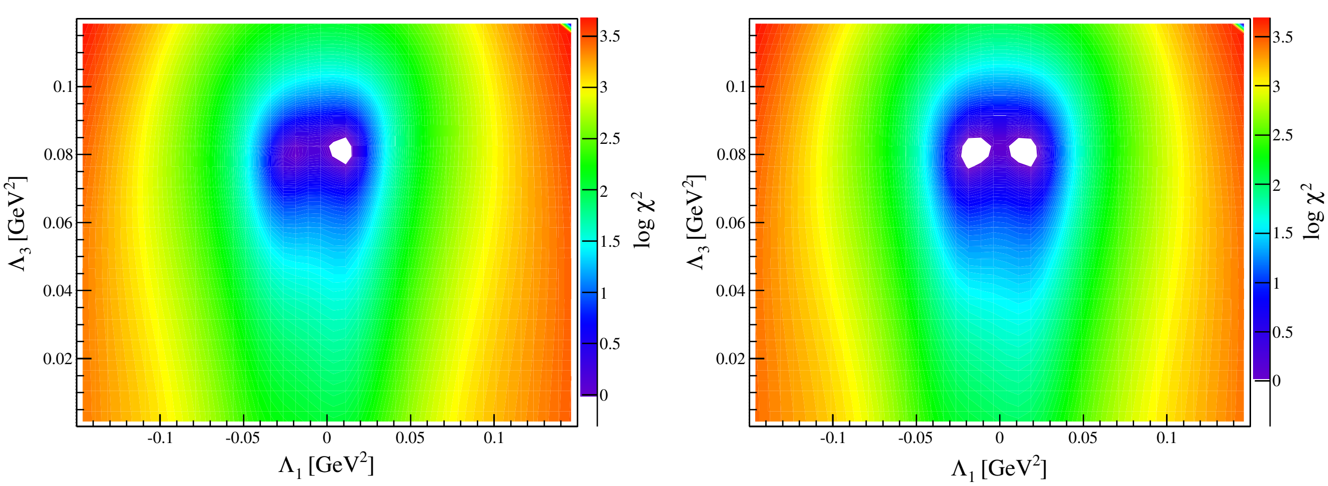

FIG. 2 (color online). χ^2 as a function of the BRpV parameters Λ_1 and Λ_3 for $\sin\alpha \approx -0.0695$ (left) and $\sin\alpha = 0$ (right), keeping the rest of the parameters as indicated in Table I.

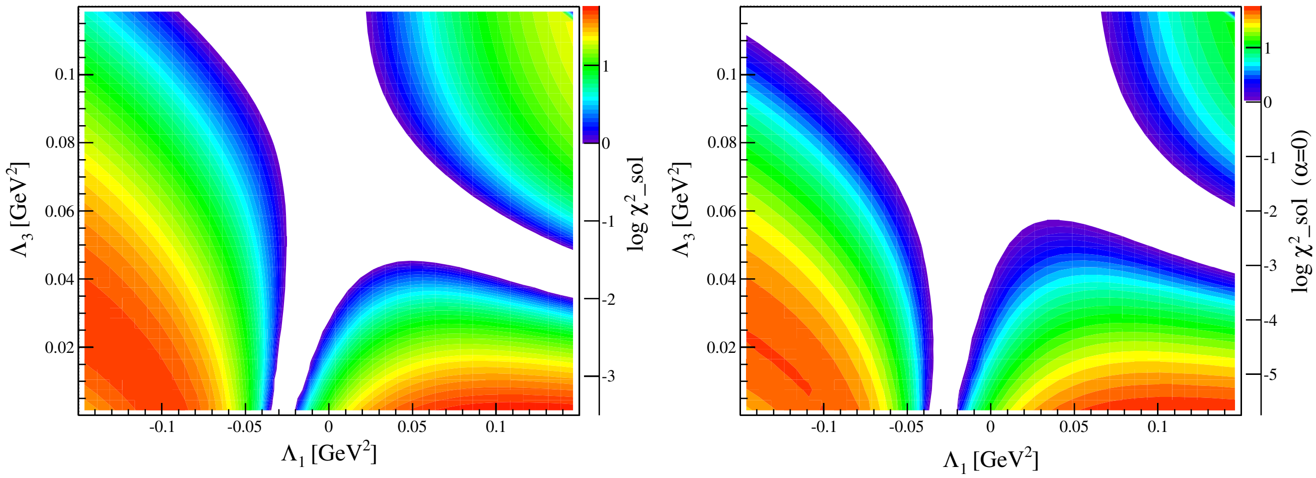

FIG. 3 (color online). $\chi^2_{s2\mathrm{sol}}$ as a function of the BRpV parameters Λ_1 and Λ_3 for $\sin\alpha \approx -0.0695$ (left) and $\sin\alpha = 0$ (right), keeping the rest of the parameters as indicated in Table I.

keeping several parameters fixed as discussed earlier, therefore, the above result should be considered as a proof of existence case rather than a generalized result.) In addition, as it can be seen from Eq. (37), an approximated symmetry under the Λ_1 sign change is reestablished in the case of $\sin\alpha = 0$. This is because in this case $\sin^2\theta_{\mathrm{rea}}$ is insensitive to this sign. In the same limit $\tan\theta_{\mathrm{atm}}$ is independent of Λ_1, while $\tan\theta_{\mathrm{sol}}$ stays sensitive to Λ_1 and its sign. In our study we restrict to positive values of $\sin(\alpha)$ but a generalization to negative values is also possible.

The previous conclusions are confirmed when we study separately the effect on χ^2 from the neutrino angles. We remind the reader that the neutrino masses are not affected by the diagonalization matrix in the charged lepton sector, as we explained below Eq. (35). In addition, the effect of the nondiagonal charged lepton matrix on the atmospheric angle is relatively small. The solar and reactor angles however get significant changes after the inclusion of charged lepton diagonalization effects. To show this we define

$$\chi^2_{s2\mathrm{sol}} = \left(\frac{\sin^2\theta_{\mathrm{sol}} - 0,315}{0,045}\right)^2, \qquad \chi^2_{s2\mathrm{rea}} = \left(\frac{\sin^2\theta_{\mathrm{rea}} - 0,018}{0,017}\right)^2, \tag{52}$$

which are the isolated contributions to χ^2 from the solar and reactor angles, respectively. In Fig. 3 we have $\chi^2_{s2\mathrm{sol}}$, with $\sin\alpha \approx -0.0695$ in the left frame and $\sin\alpha = 0$ in the right one. We see important differences in the shape of the allowed region (white). Nevertheless the overall significance is decreased because the contribution from the solar angle to χ^2 is relatively small. On the other hand, in Fig. 4 we have $\chi^2_{s2\mathrm{rea}}$ with an analogous difference between left

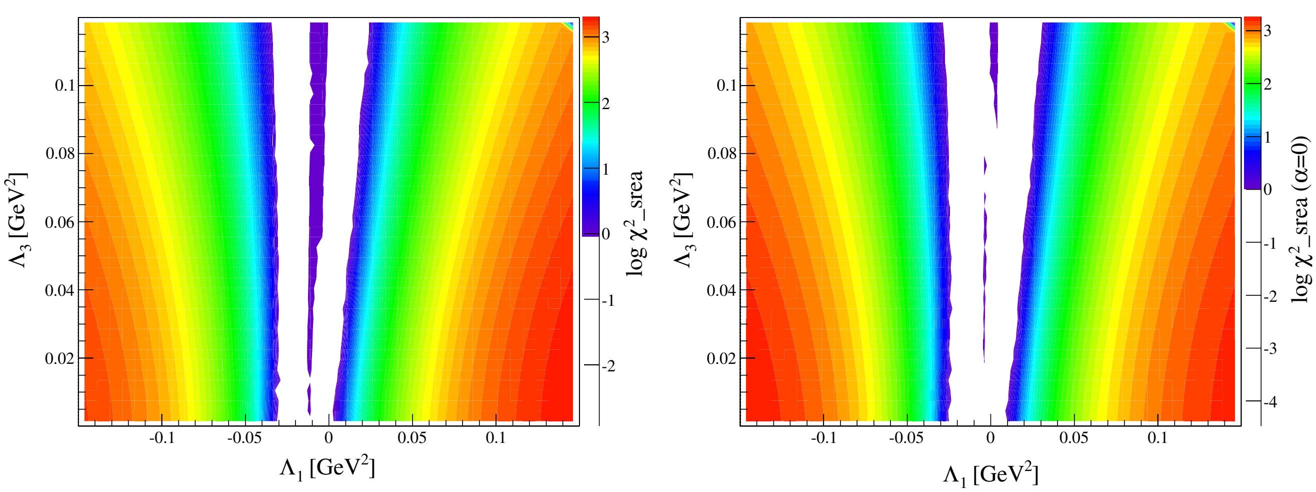

FIG. 4 (color online). $\chi^2_{s2\mathrm{rea}}$ as a function of the BRpV parameters Λ_1 and Λ_3 for $\sin\alpha \approx -0.0695$ (left) and $\sin\alpha = 0$ (right), keeping the rest of the parameters as indicated in Table I.

TABLE III. Chosen values for PSS. This values gives $\chi^2 = 0.88$.

SUSY parameters	Value	Scanned range	Units
M_1	119	[40 500]	GeV
M_2	339	[80 100]	GeV
$\lvert\mu\rvert$	456	[01000]	GeV
$\tan\beta$	5.71	[2,50]	$\cdots$
m_h	130	[114 140]	GeV
m_A	1963	[500 6000]	GeV
A	-2.73	$\cdots$	$\mathrm{eV/GeV^4}$
C	0.282	$\cdots$	$\mathrm{eV/GeV^2}$
Q	1048	$\cdots$	GeV
BRpV parameters	Value	Scanned range	Units
Λ_1	0.0317	$[-1, 1]$	$\mathrm{GeV^2}$
Λ_2	-0.0022	$[-1, 1]$	$\mathrm{GeV^2}$
Λ_3	0.0738	$[-1, 1]$	$\mathrm{GeV^2}$
ϵ_1	0.034	$[-1, 1]$	GeV
ϵ_2	0.264	$[-1, 1]$	GeV
ϵ_3	0.372	$[-1, 1]$	GeV

and right frames. The shift in the allowed region from left ($\sin\alpha \approx -0.0695$) to right ($\sin\alpha = 0$) is much smaller than in the solar angle case, but the numerical contribution to χ^2 from the reactor angle is much larger, making the reactor angle the most decisive factor in the influence of the diagonalization of the charged lepton mass matrix. One further sees that although the overall χ^2 seems to be symmetric in Λ_1 for the diagonal case, the individual contributions (especially $\sin^2\theta_{\mathrm{sol}}$) do not have such a symmetry. Thus, the fact that the "alien" in Fig. 2 closes one "eye" for the nondiagonal charged lepton matrix is actually not a general feature. We also mention that the prediction in [5] that $\mu_g = \mathcal{O}(0.01)$ eV is not affected by the scenario where the charged lepton mass matrix is not diagonal, since μ_g is in first approximation restricted only by mass differences.

TABLE IV. PSS predictions for neutrino observables given the values in Table III.

Observable	Solution	Units
$\Delta m^2_{\mathrm{atm}}$	2.43×10^{-3}	$\mathrm{eV^2}$
$\Delta m^2_{\mathrm{sol}}$	7.66×10^{-5}	$\mathrm{eV^2}$
$\sin^2\theta_{\mathrm{atm}}$	0.495	$\cdots$
$\sin^2\theta_{\mathrm{sol}}$	0.323	$\cdots$
$\sin^2\theta_{\mathrm{rea}}$	0.0026	$\cdots$

B. Partial split SUSY

In PSS the parameter space consists of, first, the supersymmetric parameters Bino mass M_1, Wino mass M_2, Higgsino mass μ, $\tan\beta$, and Higgs masses m_h and m_A, which define the constants A and C in Eq. (44); second, the BRpV parameters Λ_i and ϵ_i; and third, the charged lepton Yukawa parameters E, F, and D, which define the angles $\sin\alpha'$ and $\sin\theta'$ in (19).

As we did for the previous model, we perform a scan over parameter space and look for solutions with predictions on neutrino observables compatible with experimental data, represented by the value of $\chi^2 < 1$ as given in Eq. (51). A working scenario satisfying this criteria is given in Table III. The effect of the first 6 parameters is in the values of A and C which enter in the neutrino mass matrix. The scale Q is chosen such that there is no mixing term between Λ and ϵ. The scenario is completed with the values of the BRpV parameters Λ_i and ϵ_i. In Table IV we have the predictions for the neutrino observables in this model, which gives a value of $\chi^2 = 0.88$.

Similarly to the previous model, in Fig. 5 (left) we have the logarithm of χ^2 as contour regions in the ϵ_3-ϵ_1 plane, with all the other parameters fixed at their values in Table III, plus $\sin\alpha' = 0.070$ and $\sin\theta' = 0.036$ (In this case we have chosen positive signs). The white region corresponds to $\chi^2 < 1$, i.e. points that satisfy the experimental constraints.

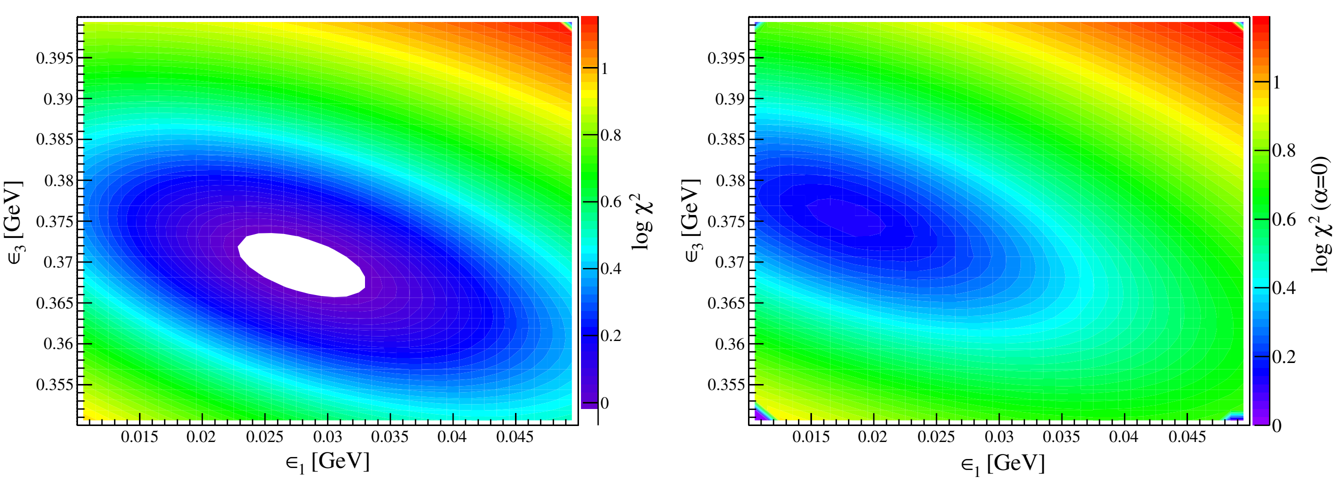

FIG. 5 (color online). χ^2 in dependence of ϵ_2 and ϵ_3, while the other parameters are fixed around the central value from Table III. On the left-hand side $\sin\alpha' = 0.070$ and $\sin\theta' = 0.036$ was used, while on the right-hand side a diagonal charged lepton matrix was used.

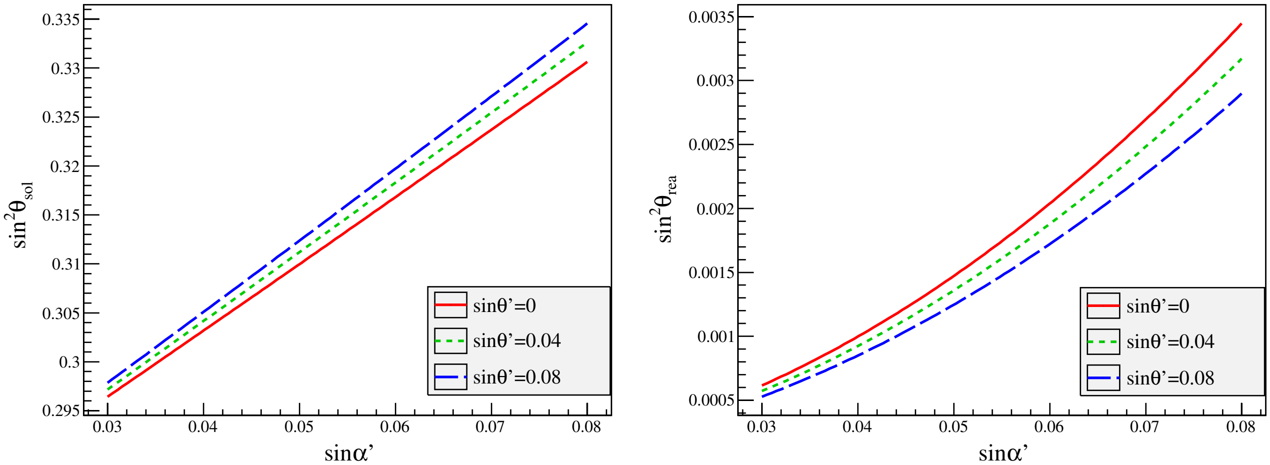

FIG. 6 (color online). $\sin^2\theta_{\rm sol}$ and $\sin^2\theta_{\rm rea}$ dependence on $\sin\alpha'$ for different values of $\sin\theta'$. The other parameters are fixed around the central values in Table III.

Neglecting the effects of the diagonalization of the charged lepton mass matrix corresponds to set $\sin\alpha' = \sin\theta' = 0$, and when this is done we find $\chi^2 = 2.81$, meaning that a good point could have been missed if the charged lepton mass matrix diagonalization had not been taken into account (Again this is done keeping several parameters fixed). This is one example where a modified charged lepton matrix, allows to include new good parameter points. Since some points are excluded and others are included the nondiagonal charged lepton matrix actually provokes a deformation of the allowed parameter space. This can be seen graphically from Fig. 5 (right) which is the analogous to the previous figure but neglecting the charged lepton mass matrix diagonalization.

It is useful to study the individual dependence of the neutrino angles on the charged lepton rotation matrix angles α' and θ'. In Fig. 6 we have solar angle (left) and reactor angle (right) as a function of $\sin\alpha'$ for three different values of $\sin\theta'$. In both cases the dependence on $\sin\alpha'$ is stronger that the dependence on $\sin\theta'$, as can be noticed from Eqs. (50), where we see that the solar and reactor angles depend at first order only on $\sin\alpha'$, and a dependency on $\sin\theta'$ appears only at second order. Although the dependency of the solar angle on $\sin\alpha'$ is strong, it variation on the chosen range for $\sin\alpha'$ maintains the solar angle within its 3σ experimental region. On the contrary, the reactor angle being also very sensitive to $\sin\alpha'$, can escape from below the experimental widow, while keeping its value well below the upper 3σ bound. Therefore, a lower bound on the reactor angle already constraints the model.

In Fig. 7 we have a similar plot for the dependence of the atmospheric angle on $\sin\theta'$ for three different values of $\sin\alpha'$. As opposed to the previous cases, for the atmospheric angle the dependence is stronger on $\sin\theta'$ rather than on $\sin\alpha'$. From Eq. (50) we see that despite the fact that $\tan\theta_{23}$ depends at first order on both angles, $\sin\alpha'$ is multiplied by the reactor angle and makes its influence much smaller. In

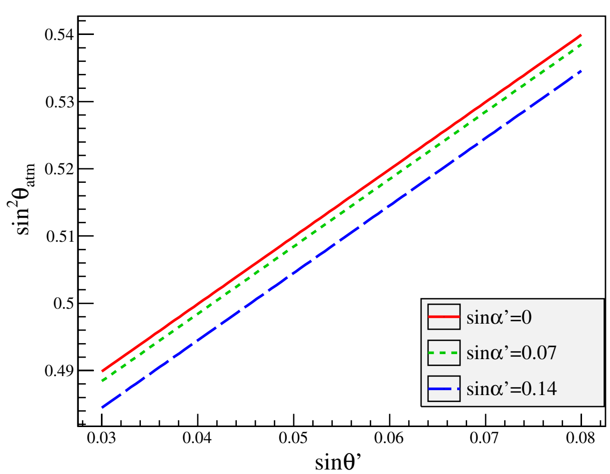

FIG. 7 (color online). $\sin^2\theta_{\rm atm}$ dependence on $\sin\theta'$ for different values of $\sin\alpha'$. The other parameters are fixed around the central values in Table III.

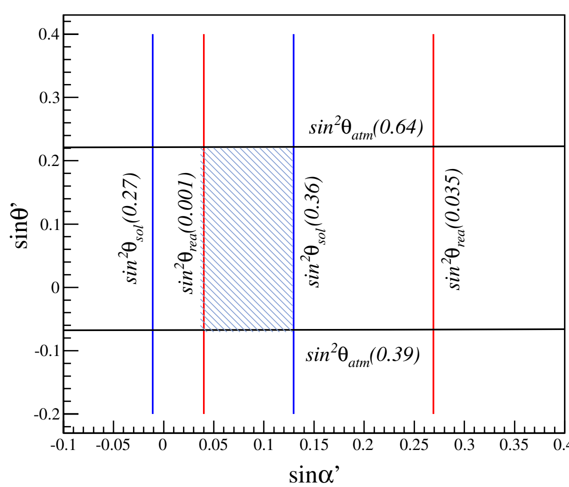

FIG. 8 (color online). Range of $\sin\theta'$ and $\sin\alpha'$ that gives $\chi^2 < 1$, for the scenario given in Table III.

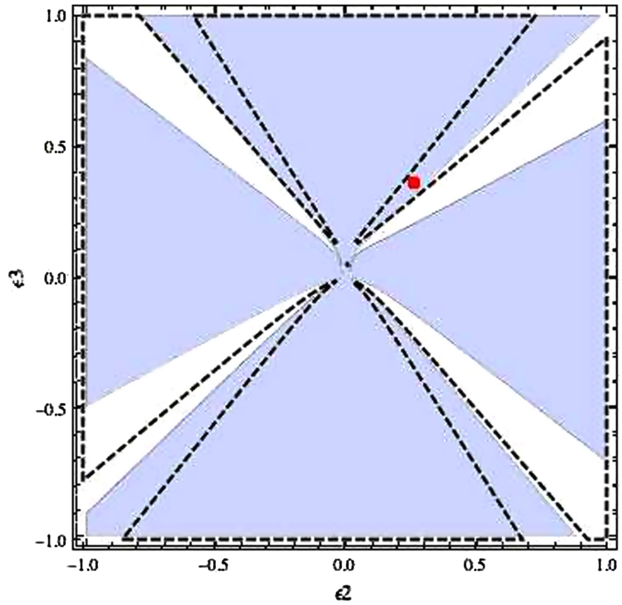

FIG. 9 (color online). $\chi^2_{s2\mathrm{sol}}$ is plotted in the (ϵ_2 [GeV], ϵ_3 [GeV]) plane for the complex parameter $\delta_{\epsilon 1} = 0.02$. The white region is $\chi^2_{s2\mathrm{sol}} < 1$ and the complementary colored region is $\chi^2_{s2\mathrm{sol}} > 1$. The dotted line shows how this contour would look like for $\delta_{\epsilon 1} = 0$. The rest of the parameters are chosen according to Table III. The red dot represents this numerical working scenario for purely real values.

any case, over the chosen range for $\sin\theta'$, the atmospheric angle does not leave the 3σ experimental window.

In a related numerical analysis we plot in Fig. 8 the allowed region (defined by $\chi^2 < 1$) in the $\sin\theta'$–$\sin\alpha'$ plane, with the effect of the different neutrino angle 3σ bounds shown as solid lines. Here we confirm that the atmospheric angle restricts the values of $\sin\theta'$, while the solar and reactor angles restrict the values of $\sin\alpha'$. The typical value for the charged lepton mixing angles in the Giudice ansatz are $\sin\theta' = 0.036$ and $\sin\alpha' = 0.07$, and θ' will start to be probed if the error in the atmospheric angle diminishes by a few times. On the other hand, the value of α' can be probed with an improvement on the lower bound of the reactor angle, and with an improvement on the upper bound of the solar angle.

C. Complex parameters

One can also allow for complex parameters in the model. A general study with complex parameters is beyond the scope of this article. Nevertheless, in order to illustrate the effects of such generalization, we allow a small set of parameters to be complex. If one allows for a complex Hermitian V_L in the charged lepton sector by replacing $F \to F \cdot e^{i\delta_F}$ and $E \to E \cdot e^{i\delta_E}$ one finds that those two phases factorize out in the U_{PMNS} matrix of our models and do not contribute to physically observable angles or phases. This changes however if one allows for complex RpV parameters, like, for example,

$$\epsilon_1 = |\epsilon_1| e^{i\delta_{\epsilon 1}}. \tag{53}$$

Please note that the procedure of integrating out the heavy fields lead to the definition of the RpV parameter $\Lambda_i = \mu b_i v_u + \epsilon_i v_d$. Thus, by virtue of (53), also Λ_1 will get a complex phase $\Lambda_1 = |\Lambda_1| e^{i\delta_\lambda} = \mu b_1 v_u + |\epsilon_1| e^{i\delta_{\epsilon 1}} v_d$. Since the influence of the ϵ parameters is small in most of the observables (notable exceptions are neutrino physics and LSP decays), we do not evaluate the effects of those complex parameters on possible observables of CP violation. In order to gain an analytical understanding we will study (53) with the approximations of the type of (49). However, since the ϵ_1 now also contains complex values one has to make sure that the matrix $U_\nu \approx (\vec{\epsilon}_1, \vec{\epsilon}_2, \vec{\epsilon}_3)$ is also unitary $U_\nu^\dagger U_\nu = U_\nu U_\nu^\dagger = 1$. This is achieved by some (partial) complex conjugations in the eigenvectors ϵ_2 and ϵ_3. A further modification with respect to the solution (49) is imposed by the numerical working scenario, which turns out to be loop dominated ($A^2|\vec{\Lambda}|^4 \ll C^2|\vec{\epsilon}|^4$). With those two adjustments the eigenvectors read

$$\vec{e}_1 = -\frac{\vec{\epsilon} \times \vec{\Lambda}}{|\vec{\epsilon} \times \vec{\Lambda}|}, \qquad \vec{e}_2 = \frac{\vec{\epsilon} \times (\vec{\Lambda} \times \vec{\epsilon})^*}{|\vec{\epsilon} \times (\vec{\Lambda} \times \vec{\epsilon})^*|}, \qquad \vec{e}_3 = \frac{\vec{\epsilon}^*}{|\vec{\epsilon}|}. \tag{54}$$

After taking into account taking into account that for complex matrices one has $U_{\mathrm{PMNS}} = V_L U_\nu^*$ [11], this approximation allows to obtain analytic expressions for the neutrino mixing angles

$$\sin(\theta_{13}) = \left|\frac{\epsilon_1 \cos(\alpha') - \epsilon_2 \sin(\alpha')}{|\vec{\epsilon}|}\right| \qquad \tan(\theta_{23}) = \left|\frac{\epsilon_2 \cos(\alpha')\cos(\theta') - \epsilon_1 \sin(\alpha')\cos(\theta') - \epsilon_3 \sin(\theta')}{\epsilon_3 \cos(\theta') + (\epsilon_2 \cos(\alpha') + \epsilon_1 \sin(\alpha'))\sin(\theta')}\right|$$

$$\tan(\theta_{12}) = \left|\frac{(\Lambda_2\epsilon_1\epsilon_2 - \Lambda_1(\epsilon_2^2 + \epsilon_3^2) + \Lambda_3\epsilon_1\epsilon_3)\cos(\alpha') + (\Lambda_2(\epsilon_1^*\epsilon_1 + \epsilon_3^2) - \Lambda_1\epsilon_1^*\epsilon_2 - \Lambda_3\epsilon_2\epsilon_3)\sin(\alpha')}{|\vec{\epsilon}|((\Lambda_3\epsilon_2 - \Lambda_2\epsilon_3)\cos(\alpha') + (\Lambda_3\epsilon_1 - \Lambda_1\epsilon_3)\sin(\alpha'))}\right|. \tag{55}$$

Those approximated solutions turn out to reproduce roughly the numeric working scenario. They work especially well for the solar angle which agrees with the numerical solution at a precision of about 1%. Since both Λ_1 and ϵ_1 became complex, the measured value of $\sin(\theta_{12})$ gets modified. This is now compared to the corresponding observable as defined in (52). As one can see in Fig. 9, the introduction of complex parameters, such as $\delta_{\epsilon 1}$ can lead to significant modifications to observable mixing angles such as $|\sin(\theta_{12})|^2$. Very similar effects would appear in the context of the previously studied gravity-motivated model where the complex phase (53) would lead to a phase of $\lambda_1 = a_1\mu + \epsilon_1$.

VIII. SUMMARY

It is a known fact that the Yukawa matrix of the charged leptons does not have to be diagonal. In order to see how the usual assumption in BRpV studies of a diagonal charged lepton Yukawa matrix affects neutrino observables, we studied the impact of a nondiagonal charged lepton Yukawa matrix on the neutrino sector of split supersymmetric models. This was done by using two different ansätze for the charged lepton matrix. It was found that the mass differences between the different neutrino species are effectively insensitive to the charged lepton sector. This confirms the usual assumption of a diagonal charged lepton matrix with this respect. However, when studying the neutrino mixing angles it was found that the form of the mass matrix of the charged leptons indeed can provoke significant changes in the observables. We found that especially the solar and reactor mixing angles are sensitive to this effect, whereas the atmospheric angle shows a somewhat weaker dependence. Thus, it has been shown that the usual assumption in BRpV analysis of a diagonal mass matrix for charged leptons, can lead to important deformation in the allowed parameter space and mistakes in the interpretation of experimental data. In other words, within given models like the ones studied in this article, a parameter point that agrees with the experimental neutrino data in the context of a diagonal charged lepton matrix, is likely to disagree with the data in the context of a nondiagonal charged lepton matrix or vice versa.

ACKNOWLEDGMENTS

The work of M. A. D. was partly funded by Conicyt Grant No. 1100837 (Fondecyt Regular). B. K. was funded by Conicyt-PBCT Grant No. PSD73.

Note added in proof.—A new measurement of the reactor angle was announced after the submission of this paper [28]. This finding is in agreement with our presented scenario.

[1] R. Barbier *et al.*, Phys. Rep. **420**, 1 (2005); H. K. Dreiner, Pramana **51**, 123 (1998).
[2] R. Hempfling, Nucl. Phys. **B478**, 3 (1996); M. Drees, S. Pakvasa, X. Tata, and T. ter Veldhuis, Phys. Rev. D **57**, R5335 (1998); E. J. Chun, S. K. Kang, C. W. Kim, and U. W. Lee, Nucl. Phys. **B544**, 89 (1999); Y. Grossman and S. Rakshit, Phys. Rev. D **69**, 093002 (2004); S. Davidson and M. Losada, J. High Energy Phys. 05 (2000) 021.
[3] M. A. Diaz, S. G. Saenz, and B. Koch, Phys. Rev. D **84**, 055007 (2011).
[4] M. A. Diaz, M. Hirsch, W. Porod, J. C. Romao, and J. W. F. Valle, Phys. Rev. D **68**, 013009 (2003); **71**, 059904(E) (2005).
[5] M. A. Diaz, B. Koch, and B. Panes, Phys. Rev. D **79**, 113009 (2009).
[6] M. A. Diaz, F. Garay, and B. Koch, Phys. Rev. D **80**, 113005 (2009).
[7] D. Restrepo, M. Taoso, J. W. F. Valle, and O. Zapata, Phys. Rev. D **85**, 023523 (2012).
[8] H. Georgi and C. Jarlskog, Phys. Lett. **86B**, 297 (1979).
[9] S. Dimopoulos, L. J. Hall, and S. Raby, Phys. Rev. D **45**, 4192 (1992).
[10] W. Krolikowski, arXiv:hep-ph/0509184.
[11] S. F. King, J. High Energy Phys. 09 (2002) 011; Rep. Prog. Phys. **67**, 107 (2004).
[12] K. Nakamura *et al.* (Particle Data Group Collaboration), J. Phys. G **37**, 075021 (2010).
[13] G. F. Giudice, Mod. Phys. Lett. A **7**, 2429 (1992).
[14] H. K. Dreiner, G. K. Leontaris, S. Lola, G. G. Ross, and C. Scheich, Nucl. Phys. **B436**, 461 (1995).
[15] G. K. Leontaris, S. Lola, C. Scheich, and J. D. Vergados, Phys. Rev. D **53**, 6381 (1996).
[16] S. K. Kang and C. S. Kim, Phys. Rev. D **63**, 113010 (2001).
[17] C. Liu, Mod. Phys. Lett. A **12**, 329 (1997); in *Frontiers of Theoretical Physics: A General View of Theoretical Physics at the Crossing of Centuries, Proceedings of the International Workshop Beijing, China, 25 November 1999*, edited by F. Sakata, K. Wu, and E.-G. Zhao (World Scientific, Singapore, 1999), p. 131.
[18] N. Arkani-Hamed and S. Dimopoulos, J. High Energy Phys. 06 (2005) 073; G. F. Giudice and A. Romanino, Nucl. Phys. **B699**, 65 (2004); **B706**, 487(E) (2005).
[19] M. A. Diaz, P. Fileviez Perez, and C. Mora, Phys. Rev. D **79**, 013005 (2009).
[20] S. Davidson and M. Losada, Phys. Rev. D **65**, 075025 (2002); Y. Grossman and S. Rakshit, Phys. Rev. D **69**, 093002 (2004).
[21] V. Berezinsky, M. Narayan, and F. Vissani, J. High Energy Phys. 04 (2005) 009.
[22] T. Schwetz, M. Tortola, and J. W. F. Valle, New J. Phys. **13**, 109401 (2011).
[23] R. Sundrum, J. High Energy Phys. 01 (2011) 062.
[24] S. Weinberg, Phys. Rev. Lett. **43**, 1566 (1979).
[25] M. Hirsch, H. V. Klapdor-Kleingrothaus, and S. G. Kovalenko, Phys. Lett. B **398**, 311 (1997).
[26] M. Maltoni, T. Schwetz, M. A. Tortola, and J. W. F. Valle, New J. Phys. **6**, 122 (2004).
[27] T. Schwetz, M. Tortola, and J. W. F. Valle, New J. Phys. **13**, 063004 (2011).
[28] F. P. An *et al.* (DAYA-BAY Collaboration), Phys. Rev. Lett. **108**, 171803 (2012); J. K. Ahn *et al.* (RENO Collaboration), arXiv:1003.1391; see also: http://www.symmetrymagazine.org/breaking/category/neutrinos/.